



HAL
open science

Terpy(Pt–salphen)₂ Switchable Luminescent Molecular Tweezers

Benjamin Doistau, Arnaud Tron, Sergey A. Denisov, Gediminas Jonusauskas,
Nathan D. McClenaghan, Geoffrey Gontard, Valérie Marvaud, Bernold
Hasenknopf, Guillaume Vives

► **To cite this version:**

Benjamin Doistau, Arnaud Tron, Sergey A. Denisov, Gediminas Jonusauskas, Nathan D. McClenaghan, et al.. Terpy(Pt–salphen)₂ Switchable Luminescent Molecular Tweezers. Chemistry - A European Journal, 2014, 20 (48), pp.15799-15807. 10.1002/chem.201404064 . hal-01103182

HAL Id: hal-01103182

<https://hal.science/hal-01103182>

Submitted on 21 Feb 2018

HAL is a multi-disciplinary open access archive for the deposit and dissemination of scientific research documents, whether they are published or not. The documents may come from teaching and research institutions in France or abroad, or from public or private research centers.

L'archive ouverte pluridisciplinaire **HAL**, est destinée au dépôt et à la diffusion de documents scientifiques de niveau recherche, publiés ou non, émanant des établissements d'enseignement et de recherche français ou étrangers, des laboratoires publics ou privés.



Distributed under a Creative Commons Attribution - ShareAlike 4.0 International License

Terpy(Pt–salphen)₂ Switchable Luminescent Molecular Tweezers**

Benjamin Doistau,^[a, b] Arnaud Tron,^[c] Sergey A. Denisov,^[c] Gediminas Jonusauskas,^[c]
Nathan D. McClenaghan,^[c] Geoffrey Gontard,^[a, b] Valérie Marvaud,^[a, b]
Bernold Hasenknopf,^{*[a, b]} and Guillaume Vives^{*[a, b]}

Dedicated to Prof. Jean-Marie Lehn on the occasion of his 75th birthday

Abstract: The design and synthesis of switchable molecular tweezers based on a luminescent terpy(Pt–salphen)₂ (1; terpy = terpyridine) complex is reported. Upon metal coordination, the tweezers can switch from an open “W”-shaped conformation to a closed “U”-shaped form that is adapted for selective recognition of cations. Closing of the tweezers by metal coordination (M = Zn²⁺, Cu²⁺, Pb²⁺, Fe²⁺, Hg²⁺) was monitored by ¹H NMR and/or UV/Vis titrations. During the titration, exclusive formation of the 1:1 complex [M(1)] was observed, without appearance of an intermediate 1:2 complex [M(1)₂]. The crystallographic structure of the 1:1 complex was obtained with Pb²⁺ and showed a distorted

helical structure. Selective intercalation of Hg²⁺ cations by the closed “U” form was observed. The tweezers were reopened by selective metal decoordination of the terpyridine ligand by using tris(2-aminoethyl)amine (tren) as a competitive ligand without modification of the Pt–salphen complex. Detailed photophysical studies were performed on the open and closed tweezers. Structured emission was observed in the open form from the Pt–salphen moieties, with a high quantum yield and a long lifetime. The emission is slightly modified upon closing with 1 equivalent of Zn²⁺ or Hg²⁺, whereas a dramatic quenching was obtained upon intercalation of additional Hg²⁺.

Introduction

The drive to miniaturize devices has led to a variety of molecular machines^[1] inspired by macroscopic counterparts; these include molecular motors,^[2] switches,^[3] shuttles,^[4] turnstiles,^[5] barrows,^[6] elevators,^[7] nanovehicles,^[8] and tweezers.^[9] However, the reversible control of properties at the molecular level remains a challenge. Designing systems sufficiently modular to permit reversible switching of optical or magnetic properties through mechanical motion is an innovative approach. Molecular tweezers are synthetic molecular receptors with an open cavity defined by two interaction sites for substrate binding, bridged by a spacer.^[9a, b] Over the last 30 years, they have received increasing attention owing to their relevance in several

fields.^[9c] On a nanoscopic level, molecular tweezers gather information in ways that mimic biological recognition and selectivity. Control of the relative orientation of recognition sites through stimulus-responsive spacers can mimic the allosteric control frequently found in natural systems such as enzymes. Recently, molecular tweezers with Pt–terpyridine (terpy) complexes as recognition units have been described.^[10] Intercalation of aromatic substrates and square-planar platinum complexes was observed with a change in emission properties. Similarly, bis(Pt–salphen) (salphen = *N,N'*-disalicylidene-*o*-phenylenediamine) luminophores tethered by a rigid linker were recently synthesized.^[11] Photophysical changes and selective responses to metal ions (particularly Pb²⁺) were observed. Some examples of switchable molecular tweezers controlled by metal coordination,^[12] pH,^[13] light,^[14] or electrons^[15] have been described in the literature.

We are particularly interested in the control of properties at the molecular level by mechanical motion. For that purpose, switchable molecular tweezers offer an alternative approach to the more synthetically demanding rotaxane-like systems. Furthermore, they offer the possibility of a double control of the physical properties thanks to the successive switch and guest intercalation (Figure 1). We have designed a system using a terpyridine ligand as a switching unit; the terpyridine is substituted at the 6 and 6'' positions by two arms bearing molecular recognition moieties based on versatile metal–salen complexes. As demonstrated by Lehn and co-workers, uncoordinated terpyridine adopts a “W”-shaped open form owing to the repulsion of the lone pairs of the nitrogen atoms.^[12b, c, 16] Upon

[a] B. Doistau, G. Gontard, Dr. V. Marvaud, Prof. Dr. B. Hasenknopf, Dr. G. Vives
Sorbonne Universités, UPMC Univ Paris 06
UMR 8232, Institut Parisien de Chimie Moléculaire
4 place Jussieu, 75005, Paris (France)
Fax: (+ 33) 1 44 27 38 41
E mail: bernold.hasenknopf@upmc.fr
guillaume.vives@upmc.fr

[b] B. Doistau, G. Gontard, Dr. V. Marvaud, Prof. Dr. B. Hasenknopf, Dr. G. Vives
CNRS, UMR 8232, Institut Parisien de Chimie Moléculaire
4 place Jussieu, 75005, Paris (France)

[c] A. Tron, Dr. S. A. Denisov, Dr. G. Jonusauskas, Dr. N. D. McClenaghan
Univ. Bordeaux, ISM (CNRS UMR 5255) & LOMA (CNRS UMR 5798)
33400 Talence (France)

[**] terpy = terpyridine, salphen = *N,N'* disalicylidene *o* phenylenediamine



Figure 1. Principle of switchable molecular tweezers with closing upon metal coordination (sphere) and substrate (disc) intercalation.

metal coordination, the terpyridine switches to a "U"-shaped closed conformation, organizing the two recognition units into an optimal geometry to bind substrates. Upon addition of a competitive ligand, the decoordination of the terpyridine unit should lead to a reopening of the tweezers and release of the guest. We are interested in using metal-salen complexes as arms as they can present luminescent, magnetic, or catalytic properties depending on the metal center. The use of square-planar Pt^{II} luminophores can engender attractive properties such as tunable excited states that are highly sensitive to the microenvironment,^[17] and Pt-salphen derivatives have been reported to exhibit high quantum efficiencies under ambient conditions.^[18] As a proof-of-principle, the current study focuses on platinum-salphen complexes, which display strong luminescence and should act as an efficient probe for guest intercalation.

The synthesis of the terpy(Pt-salphen)₂ molecular tweezers is presented below, as well as their reversible switching with different metals and their intercalation abilities. Detailed photophysical studies of the changes in luminescence upon coordination and cation binding are also described.

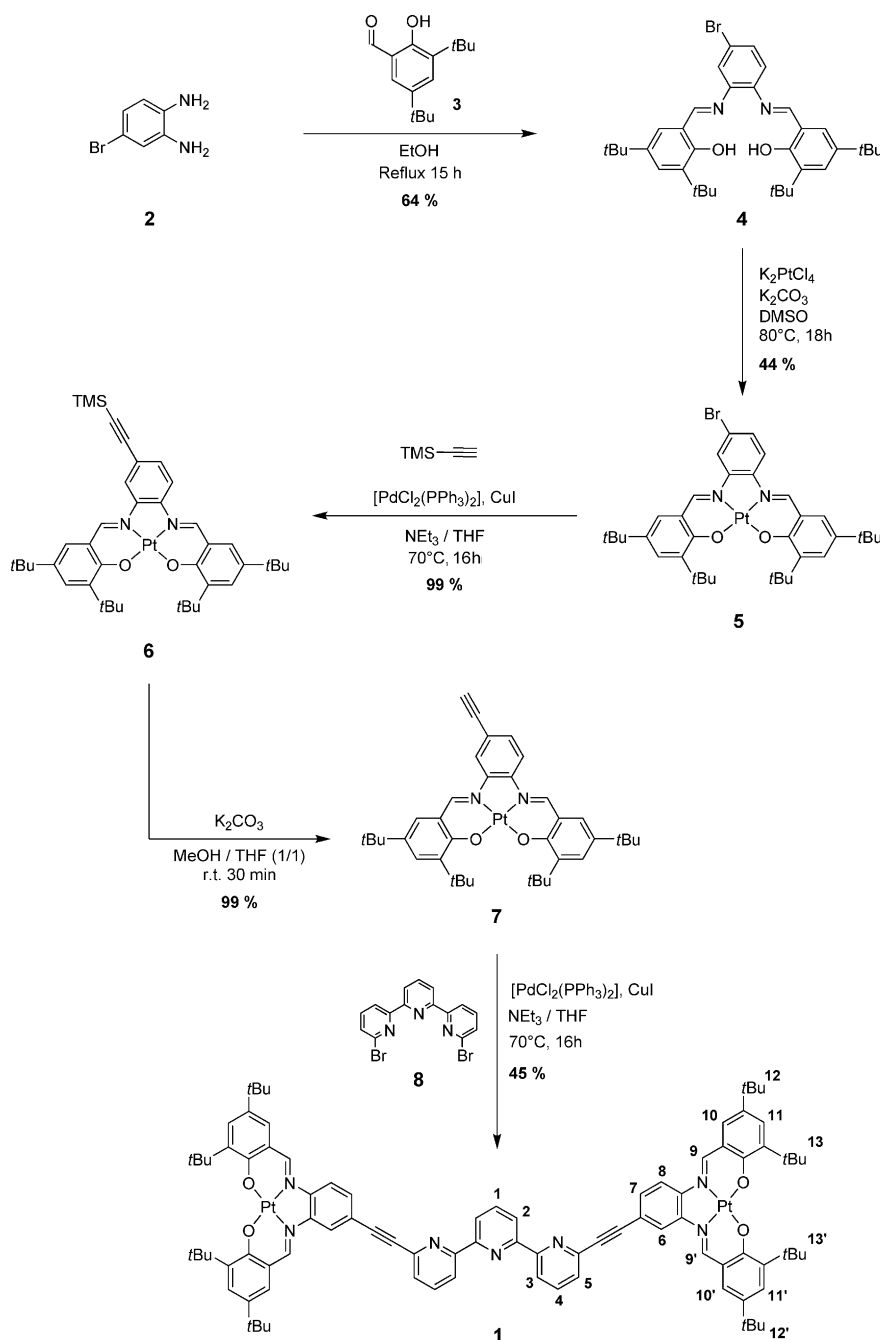
Results and Discussion

Synthesis of the molecular tweezers

The main challenge of the synthesis of **1** was to control the coordination of the two binding sites (salphen and terpyridine) and to avoid any metal exchange. As a strategy involving the synthesis of the free ligand followed by metal coordination

might lead to a mixture of products, we developed a modular strategy using a double Sonogashira coupling reaction between alkyne-substituted Pt-complex **7** and dibromoterpyridine **8** as the key step (Scheme 1). As Pt-salen complexes are known to be kinetically inert, the development of a "chemistry on complex" route was possible. *tert*-Butyl groups were introduced on the salphen moieties to increase the solubility of the final tweezers **1**, as initial attempts without them yielded insoluble products.

The synthesis started by the condensation of bromo-diaminobenzene **2** and salicylaldehyde **3** to yield salphen ligand **4**^[19] that precipitates in ethanol. Platinum was then coordinated to



Scheme 1. Synthesis of molecular tweezers **1**.

ligand **4**, by using K_2PtCl_4 as a source of Pt^{II} , to yield complex **5**. As the aryl bromide can be activated in palladium-catalyzed cross-coupling reactions, **5** was coupled with trimethylsilylacetylene (TMSA) in a Sonogashira coupling reaction followed by deprotection to obtain complex **7**. In a final step, **7** was connected to terpyridine **8** by a double Sonogashira coupling reaction yielding tweezers **1** in 45% yield. The tweezers were fully characterized by NMR spectroscopy and mass spectrometry. The non-lability of Pt-salphen complexes was confirmed during the synthesis, as no exchange between Pd^{II} and Pt^{II} was detected after the reaction.

Closing of the tweezers

Mechanical motion of the tweezers **1** was monitored by NMR and UV/Vis spectroscopy. Closing was achieved by coordination of zinc(II) to the central terpyridine ligand of the tweezers. Figure 2 shows the progressive disappearance of the free

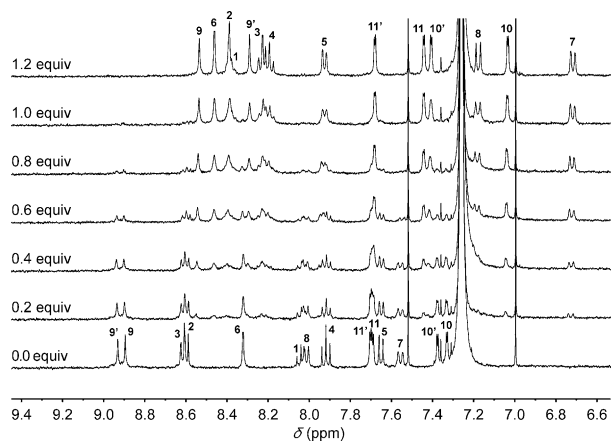


Figure 2. 1H NMR (400 MHz) titration of tweezers **1** with $Zn(SO_3CF_3)_2$ in $CDCl_3$ at 300 K.

tweezer signals in the 1H NMR spectra upon titration up to 1.0 equivalent of zinc triflate and the appearance of signals of only one new species in slow exchange on the 1H NMR timescale. Closing of the tweezers can be easily monitored by the growth of a shielded doublet at 6.7 ppm corresponding to phenyl proton H-7 (see Scheme 1 for numbering) of the $[Zn(1)]^{2+}$ complex. This complex was fully characterized by 2D NMR and mass spectrometry (Figure S30 in the Supporting Information). Two additional solvent molecules were found associated with the complex, which complete the coordination sphere of Zn^{2+} . The interaction between the terpyridine ligand and zinc was confirmed by the characteristic downfield shift of protons H-1 and H-4 in the *para*-position with respect to the nitrogen atoms.^[12c] Most of the protons of the Pt-salphen moieties and in particular proton H-7 are subject to an upfield shift, probably owing to the shielding effect of aromatic rings stacking in the "U" conformation of the tweezers. The formation of only one new species during the titration was consistent with the presence of isosbestic points ($\lambda = 587, 520, 498, 477, 404, 370,$ and 358 nm) in the UV/Vis titration at all crossing points of the

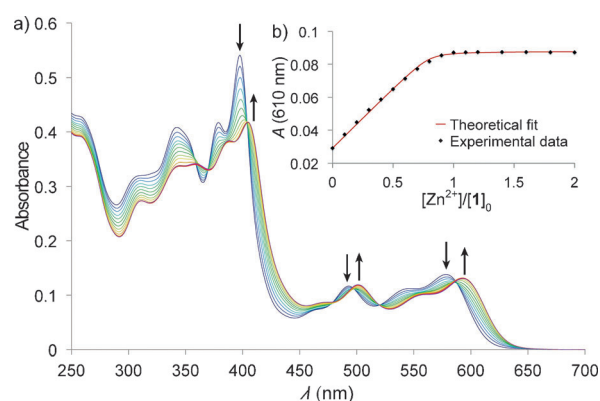


Figure 3. a) UV/Vis titration of tweezers **1** ($5.0 \times 10^{-6} \text{ mol L}^{-1}$) with $Zn(ClO_4)_2$ in $CHCl_3$. b) Absorption at 610 nm and fitting with a 1:1 binding model.

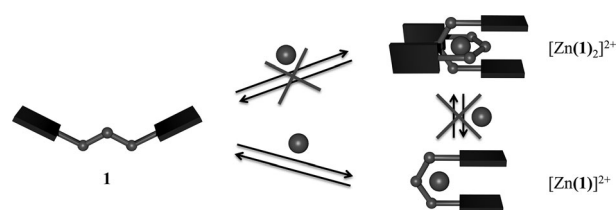


Figure 4. Tweezers **1** switching upon Zn^{2+} addition.

absorption spectra (Figure 3). Both titrations prove the evolution of the system to directly and exclusively yield the mono-terpyridine $[Zn(1)]^{2+}$ complex even at the beginning of the titration. Surprisingly, the bis-terpyridine $[Zn(1)_2]^{2+}$ complex (Figure 4), which is typically observed in the literature with the terpyridine ligand,^[16,20] was not formed, not even as an intermediate compound. This behavior is particularly attractive in the context of their use as molecular tweezers.

Indeed, this unexpected behavior was further investigated by using other metals for closing the tweezers by terpyridine coordination. The UV/Vis titrations of the tweezers **1** by metals from different blocks in the periodic table (Pb^{2+} , Fe^{2+} , Cu^{2+} , Eu^{3+} , Yb^{3+}) presented the same evolution until 1.0 equivalent, with the exclusive formation of the $[M(1)]^{n+}$ ($n = 2$ or 3) complex. UV/Vis titrations consistently gave clean isosbestic points (see Figures S15–S19 in the Supporting Information). The binding constants of the $[M(1)]^{n+}$ complexes were determined (Table S1 in the Supporting Information) by fitting absorption data with a 1:1 binding model^[21] and this revealed strong complexation constants of $\log K$ around 7 and above, even with lanthanide ions. The determination of more accurate values is not possible at the concentrations used because the fit becomes insensitive to changing the value of K . As the system behaves similarly, regardless of the metal added, the structure of the tweezers may be the cause for the non-formation of the $[M(1)_2]^{n+}$ species as an intermediate complex.

Single crystals of $[Pb(1)]^{2+}$ were obtained from $CHCl_3$ solution by slow solvent evaporation. The crystallographic structure (Figure 5) gives an insight into tweezers **1** behavior. The tweezers crystallize in a tetragonal space group (I_4) with two

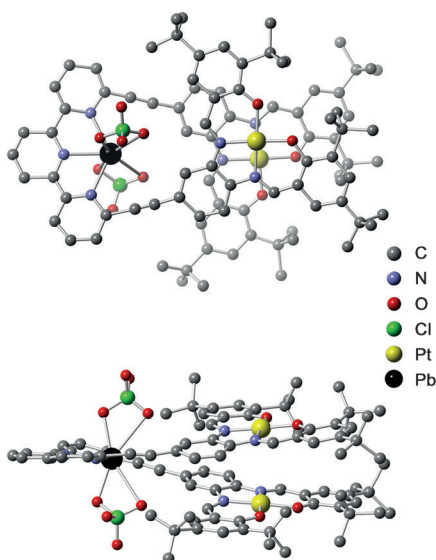


Figure 5. Top and side view of crystallographic structure of $[\text{Pb}(\mathbf{1})](\text{ClO}_4)_2$ (solvent molecules and hydrogen atoms are omitted for clarity).

molecules in the asymmetric unit of similar geometry and a large unit cell of $53.7 \times 10^3 \text{ \AA}^3$. Large channels are also observed along crystallographic axes a and b (see Figure S33 in the Supporting Information). The Pb^{2+} is bound to the terpyridine N atoms and to two O atoms of each of the two ClO_4^- counterions, resulting in the coordination number seven (distorted pentagonal bipyramidal coordination geometry). Each platinum atom displays square-planar geometry with minimal deviation of the salphen rings from the respective $\text{Pt}(\text{N}_2\text{O}_2)$ plane and average Pt–N and Pt–O distances of 1.95(2) and 1.97(2) Å, respectively, which are similar to those previously reported for Pt–salphen complexes.^[22] The terpyridine ligand adopts a twisted geometry, resulting in an unexpected stacking of the Pt–salphen moieties with an average intramolecular interplanar separation (defined as the Pt-to-Pt(N_2O_2) plane distance) of 3.73(1) Å. This distance, which is higher than in most of the Pt–salphen complexes described in the literature (~ 3.4 Å),^[22] and the non-coplanarity (angle of $10.1(7)^\circ$ on average) between the two units reveals the absence of strong π -stacking interactions probably owing to the repulsive steric effect of *tert*-butyl groups. The salphen units are almost coplanar with the terpyridine, allowing an extended electronic delocalization of the π -system through the triple bond (see Figure S34 in the Supporting Information for a representation of delocalized molecular orbitals obtained by DFT calculations) that could provide some stabilization of this conformation. Pt–Pt distances of 3.751(2) and 3.972(2) Å were observed, indicating the absence of a Pt–Pt bond, as the distance is slightly longer than the typical range ($2.7 \text{ \AA} < d < 3.5 \text{ \AA}$) for these bonds.^[23] Interestingly, the terpyridine distortion also yields a helical structure for the $[\text{Pb}(\mathbf{1})]^{2+}$ complex with the two enantiomers *P* and *M* present in the asymmetric unit, revealing no spontaneous resolution upon crystallization. This preferred conformation, if also present in solution, would cause strong steric hindrance that prevents the coordination of a second

terpyridine ligand in an orthogonal position and explains the non-formation of the $[\text{Pb}(\mathbf{1})_2]^{2+}$ complex.

Guest intercalation studies

Having achieved the tweezers' closure, the recognition of substrates by the two platinum-containing moieties was investigated. The closed form should present a new recognition site between the two phosphorescent moieties, which are pre-oriented for substrate intercalation. As the Pt^{II} is square planar, intercalation of flat aromatic molecules driven by π -stacking interactions might be observed in analogy with the bis(Pt–terpy) clips reported in the literature.^[10a,c] However, in the current case, addition of aromatic compounds of various sizes and electronic properties (anthracene, pyrene, coronene, trinitrofluorenone) to $[\text{Zn}(\mathbf{1})]^{2+}$, resulted in no clear evidence of intercalation, neither by UV/Vis nor NMR monitoring. The combination of π -stacking interactions and Pt–Pt bonds could also be an additional driving force for the intercalation of other Pt^{II} complexes as observed by Yam and co-workers in related systems.^[10b] However, the addition of Pt–salphen or Pt–porphyrin complexes to $[\text{Zn}(\mathbf{1})]^{2+}$ did not show any host/guest interactions. These observations might be explained by the steric hindrance of the *tert*-butyl groups necessary for solubility and the overlap of two Pt–salphen moieties, as revealed by the crystallographic structure of $[\text{Pb}(\mathbf{1})]^{2+}$ (Figure 5). If this twisted conformation also occurs in solution, it might prevent the intercalation of flat substrates in the same way it prevented the formation of the bis-terpyridine $[\text{Zn}(\mathbf{1})_2]^{2+}$ complex.

However, during the closing studies of tweezers **1**, a specific behavior was observed upon mercury addition. The UV/Vis titration of **1** by $\text{Hg}(\text{ClO}_4)_2$ displayed two successive evolutions (Figure 6). Up to the addition of around one equivalent of mercury, the system behaves as with other metals, with a bathochromic shift of the low-energy absorption band of the Pt–salphen unit to 620 nm and a decrease of the 400 nm band characteristic of the terpyridine coordination and closed tweezers form. As isosbestic points were observed during this titration,

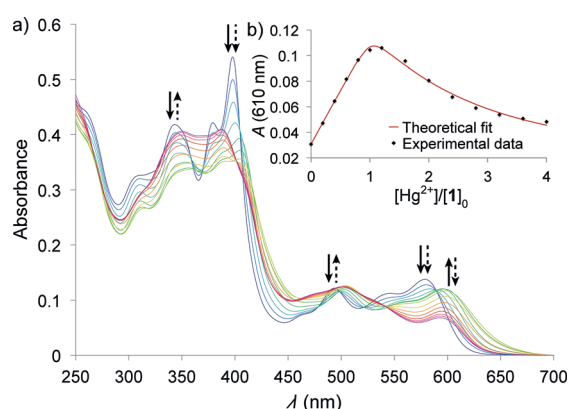


Figure 6. a) UV/Vis titration of tweezers **1** ($5.0 \times 10^{-6} \text{ mol L}^{-1}$) by $\text{Hg}(\text{ClO}_4)_2$ in CHCl_3 at 298 K. (Bold arrows: first evolution 0 to 1 equivalents; dashed arrows: second evolution 1 to 4 equivalents). b) Absorbance at 610 nm and 1:2 binding model fit.

only two species should be in the equilibrium: **1** and $[\text{Hg}(\mathbf{1})]^{2+}$. However, upon addition of more than one equivalent of mercury ions, another evolution was observed (see Figures S21 and S22 in the Supporting Information) with the appearance of new isosbestic points and a dramatic change in the absorption spectrum. The successive binding constant ($\log K_1=6.9$; $\log K_2=5.5$) were determined by fitting the UV/Vis data with a 1:2 binding model. The first complexation presents a binding constant in the same order of magnitude as for other metals, whereas a weaker binding is observed for the intercalation. The Job plot between $[\text{Hg}(\mathbf{1})]^{2+}$ and Hg^{2+} (see Figure S20 in the Supporting Information) showed a maximum at 0.5, indicating a 1:1 stoichiometry for formation of the new $[\text{Hg}_2(\mathbf{1})]^{4+}$ complex. The formation of this $[\text{Hg}_2(\mathbf{1})]^{4+}$ complex was also confirmed by mass spectrometry, with the observation of characteristic molecular peaks of $[\text{Hg}_2(\mathbf{1})\text{Cl}_2]^{2+}$ and $[\text{Hg}_2(\mathbf{1})\text{Cl}_2\text{ClO}_4]^{+}$ (see Figures S31 and 32 in the Supporting Information). As attempts to grow single crystals suitable for X-ray diffraction were unsuccessful, NMR studies were performed to further assess the location of the second Hg^{2+} cation. At room temperature, the ^1H NMR spectra of **1** showed a broadening of the signals upon addition of $\text{Hg}(\text{ClO}_4)_2$ that can be attributed to a fluxional system close to coalescence, which was not resolved upon cooling down to 220 K. However, by using HgCl_2 for the titration, well-resolved spectra were obtained (see Figure S23 in the Supporting Information) with the progressive disappearance of the free tweezer signals and the appearance of signals of the closed tweezers in slow exchange on the ^1H NMR timescale. Interestingly, the spectra of closed tweezers $[\text{Hg}(\mathbf{1})]\text{Cl}_2$ are symmetric at room- and even low temperature, showing a fast exchange between the symmetric and antisymmetric conformation of the Pt-salphen moieties. To investigate the structure of the $[\text{Hg}_2(\mathbf{1})]^{4+}$ complex, a titration was performed at 220 K by addition of $\text{Hg}(\text{ClO}_4)_2$ to a solution of the closed tweezers $[\text{Hg}(\mathbf{1})]\text{Cl}_2$. A broadening followed by a decoalescence of the signals of the aromatic and *tert*-butyl protons was observed upon addition of up to around one additional equivalent of mercury (see Figure S24 in the Supporting Information). This decoalescence might be attributed to the interaction of the second Hg^{2+} with the oxygen of one or two salphen units, thus preventing the free rotation between the two interconverting symmetric and antisymmetric conformations. As the NMR signals of the $[\text{Hg}_2(\mathbf{1})]^{4+}$ complex are broad, the precise location of the second Hg^{2+} remains difficult to determine but it should be located between the closed arms, otherwise additional mercury ions would be bound. As the H-6 and H-7 protons seem more affected by addition of the second Hg^{2+} than the H-11, H-12, and H-13 protons, we could envisage that the second Hg^{2+} was located close to the terpyridine unit, interacting with the triple bond and the aromatic cycle of the salphen and with a potential bridging perchlorate anion. However, as crystallographic structures of Hg^{2+} coordinated to the oxygen of one or two salen complexes have been reported in the literature,^[24] we presume the formation of a $[\text{Hg}\subset\text{Hg}(\mathbf{1})]^{4+}$ complex with one mercury coordinated to the terpyridine and the other coordinated to the oxygen of the Pt-salphen moieties is more likely (Figure 7). This structure is

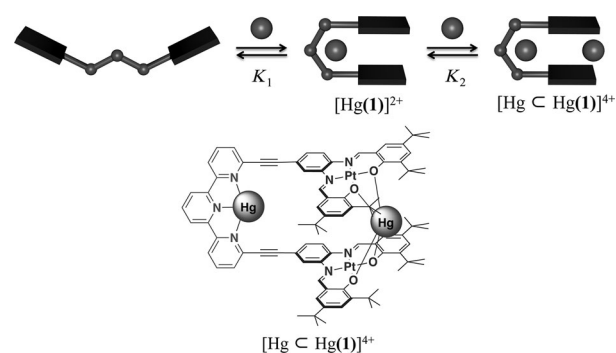


Figure 7. Successive formation of $[\text{Hg}(\mathbf{1})]^{2+}$ and $[\text{Hg}\subset\text{Hg}(\mathbf{1})]^{4+}$ complexes and proposed structure of $[\text{Hg}\subset\text{Hg}(\mathbf{1})]^{4+}$.

similar to that described previously for rigid Pt-salphen clips with Pb^{2+} .^[11b] In conclusion, the behavior of the system is consistent with a molecular tweezers action, with the intercalation of a second Hg^{2+} in the closed form, and selectivity for Hg^{2+} over Pb^{2+} .

This dynamic system is a good illustration of positive cooperativity as the metal intercalation can only occur if the tweezers are closed. Thereby, the tweezers closing upon metal coordination leads to the formation of a new binding site with four oxygen atoms, able to selectively host mercury, by an allosteric effect. Although molecular tweezers **1** can be closed upon addition of a range of metals, the intercalation of the second metal is selective for the mercury(II) cation.

Reopening studies

The reopening of the closed tweezers was studied by using a competitive ligand that coordinates the metallic center with a higher binding constant than terpyridine. Tris(2-aminoethyl)amine (tren), appears as a good candidate owing to its large binding constant with zinc and other metals described in the literature.^[25] To investigate the reversibility of closing, a ^1H NMR titration of the closed molecular tweezers $[\text{Zn}(\mathbf{1})]^{2+}$ by tren was performed (Figure 8).^[12] This titration shows the disappearance of $[\text{Zn}(\mathbf{1})]^{2+}$ complex signals and the appearance of new ones, which is typical of a system in slow exchange. The new peaks correspond exclusively to open tweezers **1**, demonstrating the lack of formation of an intermediate $[\text{Zn}(\mathbf{1})_2]^{2+}$ complex. The effective tweezers reopening was obtained after addition of around one equivalent of tren with complete recovery of ^1H NMR spectra of **1**. It should be noted that no demetalation of the Pt complex was observed upon addition of excess tren, demonstrating the stability and potential of the Pt-salphen as luminescent recognition units. The reopening of the tweezers closed with the cations used in Table S1 (in the Supporting Information) was investigated by UV/Vis titration. As expected from their similar association constants, a complete reopening and recovery of the open tweezers **1** was observed after addition of 1.0 equivalent of tren for all the cations (see Figures S25–S29 in the Supporting Information). Additionally, isosbestic points were observed, proving the presence of only two absorbing species in equilibrium and confirming the ab-

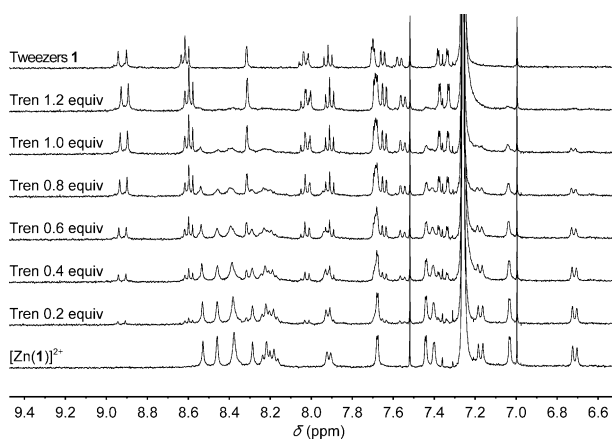


Figure 8. ^1H NMR (400 MHz) titration of the reopening of $[\text{Zn}(\mathbf{1})]^{2+}$ by tren addition in CDCl_3 at 300 K.

sence of intermediate $[\text{M}(\mathbf{1})_2]^{2+}$ complexes during the reopening.

Concerning the $[\text{Hg}\subset\text{Hg}(\mathbf{1})]^{4+}$ complex, the same reopening strategy was used. Titration with the tren ligand was performed in chloroform and monitored by UV/Vis spectroscopy (Figure 9). Two successive evolutions were observed through

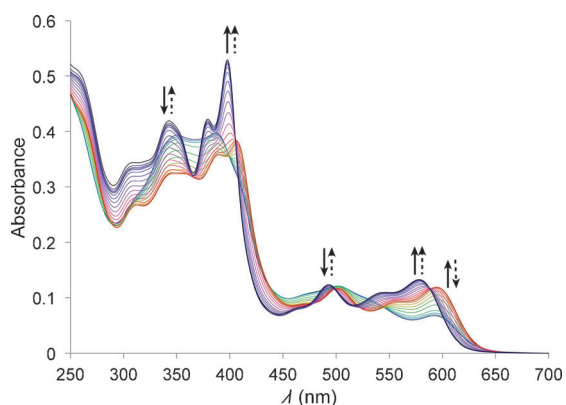


Figure 9. UV/Vis titration of the reopening of $[\text{Hg}\subset\text{Hg}(\mathbf{1})]^{4+}$ upon addition of tren (up to 4 equivalents) in CHCl_3 after closing with 4 equivalents of $\text{Hg}(\text{ClO}_4)_2$. (Bold arrows: first evolution; dashed arrows: second evolution).

this titration, with two successive series of isosbestic points. The first evolution corresponds to the removal of intercalated Hg^{2+} , followed by the mercury coordinated to the terpyridine. The successive evolutions confirm the order of the binding constant values calculated and show that the interaction of the mercury with the Pt-salphen moieties is weaker than with the terpyridine. The reversible mechanical motion of the tweezers was demonstrated by successive metal coordination and decoordination by tren addition. Moreover, this system presents advantages over photochemical switches, giving total conversion and offering thermal stability. Thus, we have been able to control the reversible mechanical motion of the tweezers and the mercury-specific recognition by taking advantage of positive cooperativity.

Photophysical studies

The impact of the closing and intercalation of some metal cations on the phosphorescence properties of the Pt-salphen moieties was investigated. We decided to focus the study on the effects of the most representative cations, that is, Zn^{2+} and Hg^{2+} . Thus, the photophysical properties of tweezers $\mathbf{1}$, $[\text{Zn}(\mathbf{1})]^{2+}$ and $[\text{Hg}(\mathbf{1})]^{2+}$, were examined by UV/Vis absorption and emission spectroscopy (Table 1). The UV/Vis absorption

Table 1. Photophysical data for tweezers $\mathbf{1}$ and complexes with Zn^{2+} and Hg^{2+} .				
Compound	λ_{abs} [nm] (ϵ [$\text{L mol}^{-1} \text{cm}^{-1}$])	λ_{em} [nm]	τ_{em} [μs] ^[a]	Φ_{em}
Tweezers $\mathbf{1}$	398 (108 000) 578 (28 000)	665	3.7	0.27
$[\text{Zn}(\mathbf{1})]^{2+}$	405 (83 000) 593 (26 000)	676	3.7	0.21
$[\text{Hg}(\mathbf{1})]^{2+}$	405 (74 000) 597 (24 000)	677	3.6	0.09
$[\text{Hg}\subset\text{Hg}(\mathbf{1})]^{4+}$	387 (82 000) 593 (14 000)	676	^[b]	$< 10^{-3}$

[a] Luminescence lifetimes at 295 K were determined on fitting experimental data to a monoexponential decay model ($\lambda_{\text{ex}} = 532 \text{ nm}$). [b] Too weak to measure accurately.

spectra of $\mathbf{1}$ in chloroform comprises bands at $\lambda < 400 \text{ nm}$ ($\epsilon > 1 \times 10^5 \text{ L mol}^{-1} \text{cm}^{-1}$) and less intense absorption bands in the visible region ($\lambda_{\text{max}} = 578 \text{ nm}$; $\epsilon = 2.8 \times 10^4 \text{ L mol}^{-1} \text{cm}^{-1}$). On comparison with the literature for phenyl-substituted analogues, the UV absorption bands can be assigned to intraligand ($\pi-\pi^*$) transitions of salphen and terpy, whereas the low-energy absorptions between 480 and 580 nm can be attributed to $\text{O}(\text{p})/\text{Pt}(\text{d}) \rightarrow \pi^*$ (diimine) charge-transfer transitions.^[18a,22] The same features are found for closed tweezers $[\text{Zn}(\mathbf{1})]^{2+}$ and $[\text{Hg}(\mathbf{1})]^{2+}$ with a bathochromic shift of 15 nm and 19 nm, respectively.

Tweezers $\mathbf{1}$ displays room-temperature emission ($\lambda_{\text{max}} = 665 \text{ nm}$) in chloroform, with a long emission lifetime ($\tau = 3.7 \mu\text{s}$), indicating phosphorescence (Figure 11, see Table 1). Upon coordination with Zn^{2+} , the relative intensity of the emission band changes with an increase at the higher energy region of the emission band, concomitant with a slight bathochromic shift with respect to the open tweezers $\mathbf{1}$ (Figure 10). The emission quantum yield of the open form ($\Phi_{\text{em}} = 0.27$) decreases ($\Phi_{\text{em}} = 0.21$) upon closing by zinc (Table 1). The same shifts of the emission spectra are observed upon coordination of one Hg^{2+} ion, with more quenching compared with zinc ($\Phi_{\text{em}} = 0.09$). The emission lifetime measured for the Pt-salphen moiety is not significantly affected by the tweezers closing (Figure 11) with zinc or mercury, despite an apparent lowering in quantum yield. However, the intercala-

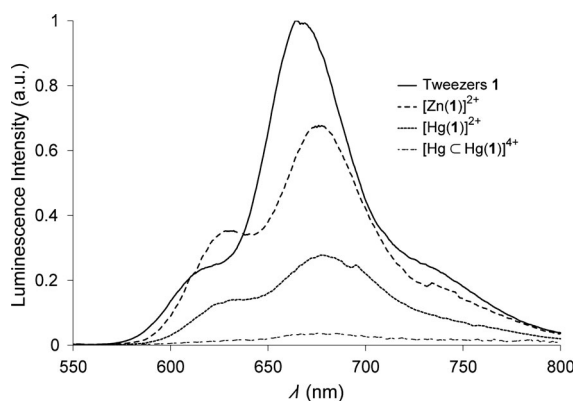


Figure 10. Emission of degassed solutions of **1**, $[\text{Zn}(\mathbf{1})]^{2+}$, $[\text{Hg}(\mathbf{1})]^{2+}$, and $[\text{Hg}\subset\text{Hg}(\mathbf{1})]^{4+}$ in CHCl_3 at 298 K ($\lambda_{\text{ex}} = 532 \text{ nm}$).

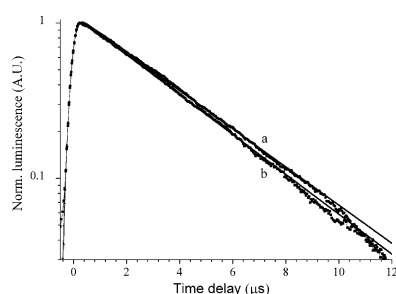


Figure 11. a) Luminescence decay for **1**. b) Luminescence decay for $[\text{Zn}(\mathbf{1})]^{2+}$. Measurements were performed in degassed dry CHCl_3 at 293 K ($\lambda_{\text{ex}} = 532 \text{ nm}$).

tion of a second mercury ion leads to a dramatic luminescence quenching ($\Phi_{\text{em}} < 10^{-3}$). Emission titration performed with mercury also shows gradual quenching and bathochromic shift of the emission (see Figure S35 in the Supporting Information).

Coordinating metal ions to the terpyridine causes a drop in emission quantum yields as new non-radiative deactivation pathways appear. As the observed lifetime does not change significantly, this implies a concomitant decrease in the radiative rate constant in what is effectively a different moiety. Indeed, transient absorption spectroscopy on the sub-nanosecond to μs scale supports this observation and kinetics observed through this technique mirror those obtained through luminescence experiments, with no evidence of participation of intervening dark states (see Figures S38–S40 in the Supporting Information). At timescales less than 10 ps, intersystem crossing was observed, and the triplet state was populated with a time constant of $\sim 140 \text{ fs}$ (see Figure S41 in the Supporting Information). Intercalation of a second mercury atom introduces a new ultrafast non-radiative deactivation channel from the Franck–Condon excited state. In this instance, excitation with visible light pulses results in rapid ground state recovery ($\tau = 250 \text{ fs}$, see Figure S42 in the Supporting Information), with no evidence for triplet state population. This rapid deexcitation is consistent with the dramatic decrease in luminescence intensity in the $[\text{Hg}\subset\text{Hg}(\mathbf{1})]^{4+}$ case. Phosphorescence lifetimes at 77 K in rigid matrix were similar (6.2 μs) for all four

samples, irrespective of whether a guest ion is present or not (see Figure S36 in the Supporting Information). This suggests a combination of thermal activation and excited-state reorganization that can potentially affect the Pt–salphen system with ion guests.

Conclusion

Molecular tweezers based on a terpyridine bis(Pt–salphen) complex have been synthesized by using a modular “chemistry on complex” strategy. The tweezers can be closed upon coordination with a large variety of metal ions and reversibly reopened by addition of the competitive tren ligand. This demonstrates the versatility of our reversible mechanical switch. Upon closing, an allosteric recognition site exhibiting selectivity for Hg^{2+} is obtained. Photophysical studies have shown that the strongly phosphorescent tweezers are only slightly modified by closing with zinc(II) or mercury(II) ions. However, a more dramatic quenching of the luminescence was obtained by intercalation of Hg^{2+} owing to sub-picosecond deexcitation pathways. This work exhibits the benefits of our molecular tweezers platform to switch physical properties at the molecular scale. Herein, the tweezers mechanical motion permits, by an allosteric effect, the formation of a new recognition site specific to mercury, the binding of which leads to the total luminescence quenching of the emissive moieties. Incorporation of the tweezers into switchable photoionic devices is envisaged, which will exploit the reversible mechanical motion at the molecular scale for sensing applications. Future work will use the versatility of the salphen ligand on the tweezers platform to control other physical properties such as magnetism or catalysis through mechanical motion.

Experimental Section

Switching studies

^1H NMR and UV/Vis titrations were performed by using distilled acetonitrile and chloroform dried over molecular sieves (4 Å) and passed through dried aluminum oxide. NMR titrations were done by successive additions of 0.2 equivalents (4 μL) of a $\text{Zn}(\text{SO}_3\text{CF}_3)_2$ solution (10 mM in $\text{CDCl}_3/\text{CD}_3\text{CN}$ (8:2)), to a solution of tweezers **1** (500 μL , 0.40 mM in CDCl_3). UV/Vis titrations were performed by successive addition of metal perchlorate solution (1.0 mM in $\text{CHCl}_3/\text{CH}_3\text{CN}$ (8:2), 0.1 equivalent, 1.5 μL), to a solution of tweezers **1** (3.0 mL, 5.0 μM in CHCl_3). These experimental conditions were chosen to minimize the amount of acetonitrile added ($< 0.4\%$) for the titrations and to maintain the solubility of the tweezers. Binding constants for 1:1 and 2:1 association were obtained by a nonlinear least-squares fit of the absorbance versus the concentration of guest added by using the Matlab program developed by P. Thordarson.^[21]

XRD crystal structure of $[\text{Pb}(\mathbf{1})](\text{ClO}_4)_2$

Single crystals were grown by slow evaporation of a mixture of chloroform/acetonitrile (8:2) of **1** (500 μL , 0.40 mM), and $\text{Pb}(\text{ClO}_4)_2$ (2.4 equivalent, 48 μL of 10 mM solution in chloroform/acetonitrile (8:2)). $\text{C}_{91}\text{H}_{99}\text{Cl}_2\text{N}_7\text{O}_{12}\text{PbPt}_2$: tetragonal, space group I_4 , a 35.7700(5) Å, b 35.7700(5) Å, c 42.0014(7) Å, α β γ 90°, V

53740.5(17) Å³, Z = 16. Intensity data were collected on a Bruker Kappa-APEXII with Cu_{Kα} micro-source radiation (λ = 1.54178 Å) at 200 K. 32968 reflections having I > 2σ(I) were used for structure determination (1.62° > θ > 57.56°). Final results: R(F) = 0.074, R_w(F) = 0.199, Gof = 1.002. CCDC-988754 contains the supplementary crystallographic data for this paper. These data can be obtained free of charge from The Cambridge Crystallographic Data Centre via www.ccdc.cam.ac.uk/data request/cif

Photophysical studies

Solutions for spectroscopic studies were degassed by multiple freeze-pump-thaw cycles and the cell was sealed with a blowtorch. Electronic absorption spectra were recorded on dilute solutions in 1 cm quartz cells by using a Varian Cary-50 spectrometer. The picosecond transient absorption set-up was built as follows. The frequency-tripled Nd:YAG amplified laser system (30 ps, 30 mJ @1064 nm, 20 Hz, Ekspla model PL 2143) output was used to pump an optical parametric generator (Ekspla model PG 401) producing tunable excitation pulses in the range 420–2300 nm. The residual fundamental laser radiation was focused in a high-pressure Xe-filled breakdown cell where a white light pulse for sample probing was produced. All light signals were analyzed by a spectrograph (Princeton Instruments Acton model SP2300) coupled with a high dynamic range streak camera (Hamamatsu C7700). Accumulated sequences (sample emission, probe without and with excitation) of pulses were recorded and treated by HPDTA (Hamamatsu) software to produce two-dimensional maps (wavelength versus delay) of transient absorption intensity in the range 300–800 nm. Typical measurement error was better than 10⁻³ O.D. This set-up was used to record luminescence decays, whereas steady-state luminescence spectra were recorded on a Horiba Jobin Yvon Fluorolog-3 spectrofluorometer equipped with a R928P PMT and were corrected. Quantum yields (Φ) of complexes were determined by comparison with an optically dilute [Ru(bpy)₃]Cl₂ (bpy = 2,2'-bipyridine) standard (Φ_{em}) in air-equilibrated water (Φ_{em} = 0.042 according to the equation: Φ = Φ_{em}(I₀I_r)(A_r/A)(η_r²/η²), where I_r refers to the reference, I is the integrated emission intensity, A is the absorbance at the excitation wavelength and η is the refractive index of the solvent.

Acknowledgements

B.D. thanks the Ecole Normale Supérieure of Cachan for a PhD Fellowship. The authors acknowledge financial support from the University of Bordeaux and Région Aquitaine. This study has been carried out in the framework of "The Investments for the Future" Programme IdEx Bordeaux - LAPHIA (ANR-10-IDEX-03-02).

Keywords: cooperativity · molecular tweezers · phosphorescence · platinum · salphen

- [1] a) V. Balzani, M. Venturi, A. Credi, *Molecular Devices and Machines: Concepts and Perspectives for the Nanoworld*, Wiley VCH, Weinheim, **2008**; b) E. R. Kay, D. A. Leigh, F. Zerbetto, *Angew. Chem.* **2007**, *119*, 72–196; *Angew. Chem. Int. Ed.* **2007**, *46*, 72–191; c) G. S. Kottas, L. I. Clarke, D. Horinek, J. Michl, *Chem. Rev.* **2005**, *105*, 1281–1376.
- [2] a) T. R. Kelly, H. De Silva, R. A. Silva, *Nature* **1999**, *401*, 150–152; b) N. Koumura, R. W. J. Zijlstra, R. A. Van Delden, N. Harada, B. L. Feringa, *Nature* **1999**, *401*, 152–155; c) D. A. Leigh, J. K. Y. Wong, F. Dehez, F. Zerbetto, *Nature* **2003**, *424*, 174–179; d) R. A. van Delden, M. K. J. ter Wiel, M. M. Pollard, J. Vicario, N. Koumura, B. L. Feringa, *Nature* **2005**, *437*, 1337–1340; e) V. Balzani, M. Clemente Leon, A. Credi, B. Ferrer, M. Venturi, A. H. Flood, J. F. Stoddart, *Proc. Natl. Acad. Sci. USA* **2006**, *103*, 1178–1183; f) G. Vives, H. P. J. de Rouville, A. Carella, J. P. Launay, G. Rapenne, *Chem. Soc. Rev.* **2009**, *38*, 1551–1561; g) U. G. E. Perera, F. Ample, H. Kersell, Y. Zhang, G. Vives, J. Echeverria, M. Grisolia, G. Rapenne, C. Joachim, S. W. Hla, *Nat. Nanotechnol.* **2012**, *8*, 46–51.
- [3] a) B. L. Feringa, *Molecular Switches*, Wiley VCH, Weinheim, **2001**; b) F. Puntoriero, F. Nastasi, T. Bura, R. Ziessel, S. Campagna, A. Giannetto, *New J. Chem.* **2011**, *35*, 948–952; c) T. Gunnlaugsson, J. P. Leonard, *Chem. Commun.* **2005**, 3114–3131.
- [4] a) N. Armaroli, V. Balzani, J. P. Collin, P. Gavina, J. P. Sauvage, B. Ventura, *J. Am. Chem. Soc.* **1999**, *121*, 4397–4408; b) A. M. Brouwer, C. Frochot, F. G. Gatti, D. A. Leigh, L. Mottier, F. Paolucci, S. Roffia, G. W. H. Worpel, *Science* **2001**, *291*, 2124–2128.
- [5] a) T. C. Bedard, J. S. Moore, *J. Am. Chem. Soc.* **1995**, *117*, 10662–10671; b) T. Lang, A. Guenet, E. Graf, N. Kyritsakas, M. W. Hosseini, *Chem. Commun.* **2010**, *46*, 3508–3510; c) T. Lang, E. Graf, N. Kyritsakas, M. W. Hosseini, *Chem. Eur. J.* **2012**, *18*, 10419–10426; d) N. Zigon, A. Guenet, E. Graf, M. W. Hosseini, *Chem. Commun.* **2013**, *49*, 3637–3639; e) N. Zigon, N. Kyritsakas, M. W. Hosseini, *Dalton Trans.* **2014**, *43*, 152–157.
- [6] a) G. Jimenez Bueno, G. Rapenne, *Tetrahedron Lett.* **2003**, *44*, 6261–6263; b) G. Rapenne, G. Jimenez Bueno, *Tetrahedron* **2007**, *63*, 7018–7026.
- [7] J. D. Badjic, V. Balzani, A. Credi, S. Silvi, J. F. Stoddart, *Science* **2004**, *303*, 1845–1849.
- [8] a) Y. Shirai, J. F. Morin, T. Sasaki, J. M. Guerrero, J. M. Tour, *Chem. Soc. Rev.* **2006**, *35*, 1043–1055; b) G. Vives, J. M. Tour, *Acc. Chem. Res.* **2009**, *42*, 473–487; c) T. Kudernac, N. Ruangsapapichat, M. Parschau, B. Macia, N. Katsonis, S. R. Harutyunyan, K. H. Ernst, B. L. Feringa, *Nature* **2011**, *479*, 208–211.
- [9] a) J. Leblond, A. Petitjean, *ChemPhysChem* **2011**, *12*, 1043–1051; b) M. Hardouin Lerouge, P. Hudhomme, M. Salle, *Chem. Soc. Rev.* **2011**, *40*, 30–43; c) F. G. Klärner, B. Kahlert, *Acc. Chem. Res.* **2003**, *36*, 919–932.
- [10] a) T. Nabeshima, Y. Hasegawa, R. Trokowski, M. Yamamura, *Tetrahedron Lett.* **2012**, *53*, 6182–6185; b) Y. Tanaka, K. Man Chung Wong, V. Wing Wah Yam, *Chem. Sci.* **2012**, *3*, 1185–1191; c) Y. Tanaka, K. M. C. Wong, V. W. W. Yam, *Chem. Eur. J.* **2013**, *19*, 390–399.
- [11] a) Z. Guo, W. L. Tong, M. C. Chan, *Chem. Commun.* **2009**, 6189–6191; b) Z. Guo, S. M. Yiu, M. C. W. Chan, *Chem. Eur. J.* **2013**, *19*, 8937–8947; c) W. L. Tong, S. M. Yiu, M. C. W. Chan, *Inorg. Chem.* **2013**, *52*, 7114–7124.
- [12] a) A. Petitjean, R. Khoury, N. Kyritsakas, J. M. Lehn, *J. Am. Chem. Soc.* **2004**, *126*, 6637–6647; b) M. Barboiu, L. Prodi, M. Montalti, N. Zaccheroni, N. Kyritsakas, J. M. Lehn, *Chem. Eur. J.* **2004**, *10*, 2953–2959; c) M. Linke Schaetzel, C. E. Anson, A. K. Powell, G. Buth, E. Palomares, J. D. Durrant, T. S. Balaban, J. M. Lehn, *Chem. Eur. J.* **2006**, *12*, 1931–1940; d) S. Ulrich, J. M. Lehn, *Chem. Eur. J.* **2009**, *15*, 5640–5645; e) S. Ulrich, A. Petitjean, J. M. Lehn, *Eur. J. Inorg. Chem.* **2010**, *2010*, 1913–1928; f) C. H. Lee, H. Yoon, W. D. Jang, *Chem. Eur. J.* **2009**, *15*, 9972–9976; g) N. C. Gianneschi, S. H. Cho, S. T. Nguyen, C. A. Mirkin, *Angew. Chem.* **2004**, *116*, 5619–5623; *Angew. Chem. Int. Ed.* **2004**, *43*, 5503–5507.
- [13] J. Leblond, H. Gao, A. Petitjean, J. C. Leroux, *J. Am. Chem. Soc.* **2010**, *132*, 8544–8545.
- [14] S. Shinkai, T. Nakaji, T. Ogawa, K. Shigematsu, O. Manabe, *J. Am. Chem. Soc.* **1981**, *103*, 111–115.
- [15] a) A. Iordache, M. Oltean, A. Milet, F. Thomas, B. Baptiste, E. Saint Aman, C. Bucher, *J. Am. Chem. Soc.* **2012**, *134*, 2653–2671; b) A. Iordache, M. Retegan, F. Thomas, G. Royal, E. Saint Aman, C. Bucher, *Chem. Eur. J.* **2012**, *18*, 7648–7653; c) B. Habermeyer, A. Takai, C. P. Gros, M. El Ojajmi, J. M. Barbe, S. Fukuzumi, *Chem. Eur. J.* **2011**, *17*, 10670–10681; d) M. Skibiński, R. Gómez, E. Lork, V. A. Azov, *Tetrahedron* **2009**, *65*, 10348–10354.
- [16] M. Barboiu, Y. M. Legrand, L. Prodi, M. Montalti, N. Zaccheroni, G. Vaughan, A. van der Lee, E. Petit, J. M. Lehn, *Eur. J. Inorg. Chem.* **2009**, *2009*, 2621–2628.
- [17] K. M. C. Wong, V. W. W. Yam, *Acc. Chem. Res.* **2011**, *44*, 424–434.
- [18] a) C. M. Che, S. C. Chan, H. F. Xiang, M. Chan, Y. Liu, Y. Wang, *Chem. Commun.* **2004**, 1484–1485; b) J. Zhang, F. Zhao, X. J. Zhu, W. K. Wong, W. Y. Wong, D. Ma, *J. Mater. Chem.* **2012**, *22*, 16448–16457; c) W. Wu, J. Sun, S. Ji, W. Wu, J. Zhao, H. Guo, *Dalton Trans.* **2011**, *40*, 11550–11561.

- [19] M. Zintl, F. Molnar, T. Urban, V. Bernhart, P. Preishuber Pflugl, B. Rieger, *Angew. Chem.* **2008**, *120*, 3508–3510; *Angew. Chem. Int. Ed.* **2008**, *47*, 3458–3460.
- [20] R. Dobrawa, M. Lysetska, P. Ballester, M. Grunea, F. Wurthner, *Macromolecules* **2005**, *38*, 1315–1325.
- [21] P. Thordarson, *Chem. Soc. Rev.* **2011**, *40*, 1305–1323.
- [22] C. M. Che, C. C. Kwok, S. W. Lai, A. F. Rausch, W. J. Finkenzeller, N. Zhu, H. Yersin, *Chem. Eur. J.* **2010**, *16*, 233–247.
- [23] a) A. Poater, S. Moradell, E. Pinilla, J. Poater, M. Sola, M. A. Martinez, A. Llobet, *Dalton Trans.* **2006**, 1188–1196; b) W. B. Connick, L. M. Henling, R. E. Marsh, H. B. Gray, *Inorg. Chem.* **1996**, *35*, 6261–6265.
- [24] a) S. Biswas, R. Saha, A. Ghosh, *Organometallics* **2012**, *31*, 3844–3850; b) L. K. Das, R. M. Kadam, A. Bauza, A. Frontera, A. Ghosh, *Inorg. Chem.* **2012**, *51*, 12407–12418.
- [25] G. Anderegg, V. Gramlich, *Helv. Chim. Acta* **1994**, *77*, 685–690.